



# THE PRE-ONSET, TRANSITIONAL, AND FOOT REGIONS IN RESISTANCE VERSUS TEMPERATURE BEHAVIOR IN HIGH- $T_c$ CUPRATES: INFERENCES REGARDING MAXIMUM $T_c$

G. C. VEZZOLI, M. F. CHEN and F. CRAVER  
U.S. ARMY MATERIALS TECHNOLOGY LABORATORY  
CERAMICS RESEARCH BRANCH

T. BURKE

U.S. ARMY ELECTRONICS, TECHNOLOGY AND DEVICES LABORATORY  
FORT MONMOUTH, NJ

W. STANLEY  
MAINSTREAM SOFTWARE  
WALTHAM, MA

September 1992

Approved for public release; distribution unlimited.



US ARMY  
LABORATORY COMMAND  
MATERIALS TECHNOLOGY LABORATORY

U.S. ARMY MATERIALS TECHNOLOGY LABORATORY  
Watertown, Massachusetts 02172-0001

92-30121



328-586

92 11 24 011

The findings in this report are not to be construed as an official Department of the Army position, unless so designated by other authorized documents.

Mention of any trade names or manufacturers in this report shall not be construed as advertising nor as an official indorsement or approval of such products or companies by the United States Government.

#### DISPOSITION INSTRUCTIONS

Destroy this report when it is no longer needed.  
Do not return it to the originator.

## UNCLASSIFIED

SECURITY CLASSIFICATION OF THIS PAGE (When Data Entered)

REPORT DOCUMENTATION PAGE		READ INSTRUCTIONS BEFORE COMPLETING FORM
1. REPORT NUMBER MTL TR 92-67	2. GOVT ACCESSION NO.	3. RECIPIENT'S CATALOG NUMBER
4. TITLE (and Subtitle) THE PRE-ONSET, TRANSITIONAL, AND FOOT REGIONS IN RESISTANCE VERSUS TEMPERATURE BEHAVIOR IN HIGH- $T_c$ CUPRATES: INFERENCES REGARDING MAXIMUM $T_c$		5. TYPE OF REPORT & PERIOD COVERED Final
7. AUTHOR(s) G. C. Vezzoli, T. Burke,* M. F. Chen, F. Craver, and W. Stanley†		6. PERFORMING ORG. REPORT NUMBER
9. PERFORMING ORGANIZATION NAME AND ADDRESS U.S. Army Materials Technology Laboratory Watertown, Massachusetts 02172-0001 ATTN: SLCMT-EMC		8. CONTRACT OR GRANT NUMBER(s)
11. CONTROLLING OFFICE NAME AND ADDRESS U.S. Army Laboratory Command 2800 Powder Mill Road Adelphi, Maryland 20783-1145		10. PROGRAM ELEMENT, PROJECT, TASK AREA & WORK UNIT NUMBERS
14. MONITORING AGENCY NAME & ADDRESS (if different from Controlling Office)		12. REPORT DATE September 1992
		13. NUMBER OF PAGES 20
		15. SECURITY CLASS. (of this report) Unclassified
		15a. DECLASSIFICATION/DOWNGRADING SCHEDULE
16. DISTRIBUTION STATEMENT (of this Report)  Approved for public release; distribution unlimited.		
17. DISTRIBUTION STATEMENT (of the abstract entered in Block 20, if different from Report)		
18. SUPPLEMENTARY NOTES *U.S. Army Electronics, Technology & Devices Laboratory, Fort Monmouth, NJ †Mainstream Software, Waltham, MA		
19. KEY WORDS (Continue on reverse side if necessary and identify by block number) Superconductivity                      Magnetic fields                      Magnetic fluxoids Supercurrent                              Kinetics                                  Flux - density Cooper pairs                                Hall effect		
20. ABSTRACT (Continue on reverse side if necessary and identify by block number)  (SEE REVERSE SIDE)		

Block No. 20**ABSTRACT**

We have studied the pre-onset deviation-from-linearity region, the transitional regime, and the foot region in the resistance versus temperature behavior of high- $T_c$  oxide superconductors, employing time varying magnetic fields and carefully controlled precise temperatures. We have shown that the best value of  $T_c$  can be extrapolated from the magnetic field induced divergence of the resistance versus inverse absolute temperature data as derived from the transitional and/or foot regions. These data are in accord with results from previous Hall effect studies. The pre-onset region however, shows a differing behavior (in  $R$  versus  $1000/T$  as a function of  $B$ ) which we believe links it to an incipient Cooper pairing that suffers a kinetic barrier opposing formation of a full supercurrent. This kinetic dependence is believed to be associated with the lifetime of the mediator particle. This particle is interpreted to be the virtual exciton formed from internal-field induced charge-transfer excitations which transiently neutralize the multivalence cations and establish bound holes on the oxygens.

# CONTENTS

	Page
INTRODUCTION . . . . .	1
EXPERIMENTAL . . . . .	1
EXPERIMENTAL RESULTS AND INTERPRETATIONS	
The Transitional and Foot Regions . . . . .	1
The Pre-onset Region in $Y_{0.5}Gd_{0.5}Ba_2Cu_3O_{7-\delta}$ and $Y_1Ba_2Cu_3O_{7-\delta}$ . . . . .	2
The Zero Resistance Region Time Dependence of Flux Readmission. . . . .	3
CONCLUSIONS AND INFERENCES . . . . .	4
REFERENCES . . . . .	17

DTIC QUALITY INSPECTED 4

Accession For	
NTIS	<input checked="" type="checkbox"/>
DTIC TAB	<input type="checkbox"/>
Unannounced	<input type="checkbox"/>
Justification	
By	
Distribution/	
Availability Codes	
Dist	Avail and/or Special
A-1	

## INTRODUCTION

Since the discovery of high- $T_c$  superconductivity,<sup>1,2</sup> the vast majority of research on the subject has concentrated on the normal state behavior (the region where the resistance,  $R$ , versus temperature,  $T$ , curve is linear), and on the zero resistance state. In contrast, much of our own work during the past two years has focused on the nonequilibrium nonquiescent zones of the  $R$  versus  $T$  behavior; these zones include what is referred to as the pre-onset region which starts where the  $R$  versus  $T$  data first begins to deviate from linearity at  $T_0$ , the transitional region in which the  $R$  versus  $T$  curve reflects nearly a vertical slope beginning near  $T_c$ , and the foot (sometimes called "tail") region in which the slope undergoes a marked change to a much lower and varying value, connecting eventually with the zero resistance region. These regions are shown in Figure 1A. The structure of the parent material  $Y_1Ba_2Cu_3O_{7-\delta}$  is given in Figure 1B, and compared to another high- $T_c$  superconductor  $Tl_1Ca_1Ba_2Cu_2O_{7-\delta}$  to show commonality of pyramidal building blocks, and also to the well known  $A_2BX_4$  related archetype. The structure of  $Y_{0.5}Gd_{0.5}Ba_2Cu_3O_{7-\delta}$  is the same as what is given in Figure 1B (left) with  $Gd^{3+}$  occupying 1/2 of the  $Y^{3+}$  sites.

## EXPERIMENTAL

We have prepared samples of  $Y_1Ba_2Cu_3O_{7-\delta}$ ,  $Y_{0.5}Gd_{0.5}Ba_2Cu_3O_{7-\delta}$ ,  $Y_1Ba_2-(Cu_{1-x}Ga_x)_3O_{7-\delta}$  and  $Bi_2Ca_2Sr_2Cu_3O_{10}$  by conventional ceramic solid-state mixing, calcining, sintering, and annealing processing.<sup>3a-c</sup> We have measured transport properties of these samples using specimen geometry in the form of rectangular solids (cut by a diamond wheel to 3 mm x 1 mm x 1.5 mm) employing four-terminal electrical resistance measurements with highly accurately controlled temperatures, and through the use of the MIT Bitter Magnet with the manual or sweep control of the field to 20T. Reference 3b describes the apparatus and precision of temperature and field control in detail. In the present study, we employed both silver and platinum epoxied electrodes (giving similar results). Reference 3c shows that resistance versus temperature curves in ceramic samples are essentially independent of contacts as long as the accepted (Ref. 3a-c) processing techniques of calcining, sintering and annealing are employed. Our samples showed single phase physical characterization to the accuracy of X-ray diffraction analysis techniques. The only exception was the 2223 composition which showed two additional phases in low concentration unless prepared by rapid solidification from the melt whereby the yield gave only the single phase (Ref. 3d). We utilized 99.9999 percent pure precursor chemicals. In past experience trace impurities that were not deliberately doped into the lattice, but were derived from lower purity precursor oxide and carbonates showed no significant effect on the resistance versus temperature data.

## EXPERIMENTAL RESULTS AND INTERPRETATIONS

### The Transitional and Foot Regions

Figures 2A and 2B give for  $Bi_2Sr_2Ca_2Cu_3O_{10}$  the resistance versus inverse absolute temperature data for respectively the transitional and the foot regions in the  $R$  versus  $T$  behavior, including dependence upon applied magnetic field. (The data in Figure 2A are derived by reducing the new data shown in the inset to the figure). These measurements extrapolate to intersection

at 114 K which agrees with the temperature at which the positive Hall coefficient versus temperature descends rapidly for the 2223 phase (shown in Figure 3).<sup>4</sup> These data then specify  $T_C$  as that temperature at which the imposition of a magnetic field (greater the  $H_{c1}$ ) creates the divergence of the  $R$  versus  $1000/T$  data. Thus the transitional regime is clearly associated with a degree of the Cooper pairing process that is triggered at, and associated with, the critical temperature  $T_C$ . The structures of Figures 2A and 2B are sufficiently different to indicate that although both the transitional and foot regions are related to a phenomenon which is statistically favored at  $T_C$ , nonetheless, these regions must reflect very differing contributing factors as well (to account for the marked differences in Figures 2A and 2B).

### The Pre-onset Region in $Y_{0.5}Ga_{0.5}Ba_2Cu_3O_{7-\delta}$ and $Y_1Ba_2Cu_3O_{7-\delta}$

Figure 4 shows magnetic field sweep (period = 60 sec) experiments taken isothermally at temperatures in the pre-onset region. The location of this region was pinpointed both by seeking the temperatures at which the magnetic field sweep (to 20T) caused an increase in the 4-terminal electrical resistance, and also by measuring the accurate  $R$  versus  $T$  data at zero magnetic field under equilibrium conditions (Figure 1). The inset to Figure 4 gives the change in resistance during a 30 sec sweep from  $B=0$  to  $B=20T$  as a function of a very accurately controlled ( $\pm 0.05$  K) temperature. Inspection of this inset figure shows a straight line containing the data points which are related to the normal state, the pre-onset region, and the transitional zone. The data points for the  $R=0$  and the foot regions falls off of this straight line. In that the pre-onset data points link via a straight line the normal and transitional state data points, we then interpret this figure to indicate that, in the pre-onset zone, Cooper pairing has already begun but has not proceeded in high enough a concentration to create a sharp resistance drop. Another way of interpreting this insufficient concentration is to hypothesize that in the pre-onset zone the lifetime of the mediator is insufficient to cause ample Cooper pairing to induce a transition to a supercurrent regime. Although the pre-onset characteristic of deviation from linearity in  $R$  versus  $T$  is shown more clearly in polycrystalline ceramic materials than in single crystals, there is no evidence to indicate that typical nonmagnetic impurities have any effect on the gross structures of  $R$  versus  $T$  or on  $T_C$  or  $T_{R=0}$ . The enhancing of charge transport nonlinearities and anomalies observed in ceramic materials is related to the effects of grain boundaries in accentuating carrier scattering processes. The nonlinearities in  $R$  versus  $T$  have not changed significantly since the early high- $T_C$  samples in which purity was far inferior to the high- $T_C$  materials prepared by current improved processing.

Figure 5 shows the  $R$  versus  $1000/T$  data for the pre-onset region of the  $R$  versus  $T$  curve as affected by the applied magnetic field. This figure contrasts the counterparts for the transitional and foot zones (Figures 2A and 2B) in that Figure 5 there is no sign of convergent extrapolation except for low fields ( $\leq 5.5T$ ). From Figure 1, we can see that the pre-onset region meets the transitional region at about 85 K ( $\approx T_C$ ), therefore the convergence at low field in Figure 5 at  $T \approx 93$  K relates to a phenomenon occurring at  $T > T_C$ , i.e., at  $T_0$ , the pre-onset temperature. The obvious difference between Figure 5 and Figure 2 indicated that there is a subtle difference between (the processes/or the stage of the processes) at work in the pre-onset zone and at work in the transitional region. This suggests that  $T_C$  may be a kinetically related phenomenon.

A further indication that the pre-onset region relates to the Cooper pairing process is the experimental observation<sup>6</sup> that the pre-onset temperature ( $T_0$ ) and the entire pre-onset zone is strongly affected (enhanced) by the spin and the effective magnetic moment of the rare earth ion that is substituted for Y in  $Y_1Ba_2Cu_3O_{7-\delta}$ . This modification is in the form of an elevation in  $T_0$  as shown in Figures 6A and 6B. These figures also show a small elevation in the temperature at which zero resistance ( $T_{R=0}$ )<sup>6,7</sup> begins, also relating to spin and effective magnetic moment. In low- $T_c$  materials, however, the effect of the spin and magnetic moment of the rare earth substituting ions is to oppose rather than enhance superconductivity-related properties as shown in Figure 6C for the rare earth added to lanthanum.<sup>8</sup> The enhancing effect of spin and magnetic moment for high- $T_c$   $Y_1Ba_2Cu_3O_{7-\delta}$  is attributed to indirect exchange forces between the moment of the center rare earth ion and the moment of the  $d^9$  Cu ion that causes a fluctuation from antiferromagnetism (Ref. 4 and 6). For the  $La_{1.8}Sr_{0.2}CuO_4$  system the addition of the rare earths (lanthanides) has a similar effect on  $T_0$  but a differing effect on  $T_{R=0}$ . This is shown in Figure 6D.<sup>9</sup>

More specifically we interpret the elevation of  $T_0$  in Figures 6A, 6B, and 6D to be a consequence of the paramagnetic moment and the spin of the centrosymmetric ion on a  $Cu^{2+}d^9$  ion whose spin is not compensated antiferromagnetically (what is referred to as a spin fluctuation from antiferromagnetism). Such a condition is established when charge balance in a  $O_{7-\delta}$  stoichiometry (of  $Y_1Ba_2Cu_3O_{7-\delta}$ ) dictates that a fraction of the chain  $Cu(1)^{3+}$  ions enter a  $Cu(1)^{2+}$  state and upset the delicately balanced antiferromagnetism of the planar region of the unit cell. The interaction between the spin of the central rare earth and the spin of the spin-fluctuation state occurs via indirect exchange and has been analyzed by a Rudderman-Kittel type approach.<sup>6</sup> This correlation causes ordering through a spin density wave.<sup>6</sup>

One further indication of the kinetic characteristics of the pre-onset region is the observation of small low-frequency oscillations<sup>4,6</sup> that commence at  $T_0$  as shown in Figure 7. These type of oscillations have been observed much earlier in low- $T_c$  materials and attributed therein to fluctuations in domain properties.<sup>10</sup> The instabilities associated with oscillations shown in Figure 7 are interpreted herein to be related to the processes of virtual exciton formation and virtual exciton ionization which respectively promote on the one hand, and breakdown, on the other hand the Cooper pairing regime.

### The Zero Resistance Region Time Dependence of Flux Readmission

We have conducted a preliminary study of the recovery of electrical resistance in  $Y_1Ba_2Cu_{3-x}Ga_xO_{7-\delta}$  using magnetic field sweep studies (in characterizing this polycrystalline material energy dispersive spectroscopy measurements show Ga weight percent  $0.5 \pm 0.3$ , for  $x=0.2$  to  $0.8\%$ , and further characterization by induced electron emission tentatively suggests that  $Ga^{3+}$  substitutes for  $Cu^{3+}$  at chain sites).<sup>11</sup> The material shows strong levitation, high density, very low porosity, large grain size, and very high electrical conductivity in the normal state. In Figure 8 we plot new data on the recovery of electrical resistance at 83.7 K in the zero resistance state as a function of the sweep rate of the magnetic field intensity. The data show that the effect of rate is most clearly observed at low field where the response of resistance recovery is lowest for the fastest sweep rate (18T in 30 sec). Thus for the most rapid sweep rate the resistive properties were not restored until a magnetic field of 1.5T was exceeded. The time response for resistance recovery is about 1 sec. This kinetic parameter or



dependence is in keeping with a phase transition phenomenon and is thought to be associated with field-induced fluxoid depinning time criteria as related to the pinning property of defects. Additional Ga substituted samples yielded the same or similar results, however, substitution of In for Ga caused the loss of superconductivity. This may be due to the absence of multivalence in indium.<sup>4,6</sup>

## CONCLUSIONS AND INFERENCES

From this study we conclude the following:

1. The governing mechanistic physics of the pre-onset regime relates to Cooper pairing and bridges the normal and transitional states. We infer that the pre-onset regime reflects time-dependent characteristics that suggest if a kinetic barrier could be overcome, then  $T_c$  could be elevated to the neighborhood of  $T_0$ .
2. The transitional and foot regions are influenced by differing phenomena but both contain characteristics that relate directly to  $T_c$  [based on  $T_c$  being interpreted as that temperatures where the B field ( $H_{c1}$ ) causes divergence of the R versus  $1000/T$  data]. However, the transitional and pre-onset regions are governed by subtly differing processes or different stages of the same process.
3. The foot region and the zero resistance state relate to each other but do not directly relate to the pre-onset region and we infer that they are not reflective of the same statistical mechanics observed in the pre-onset region.
4. From inspection of R versus T data in the R. E. BaCuO and BiCaSrCuO systems the highest possible values of  $T_c$  indicated by this study are 160 to 220 K provided chemical processing and/or catalyses can satisfy mediator lifetime criteria, believed to be related to the temperature dependence of the lifetime of the virtual exciton or charge transfer excitation.

### Note Added in Proof

It has come to the authors attention that recent work has addressed Ce and Tb substitution for Y in  $Y_1Ba_2Cu_3O_{7-\delta}$  including the effect on the R versus T curves (Ref 12). This work has shown that for  $Y_{0.5}Tb_{0.5}Ba_2Cu_3O_7$  and for  $Y_{0.75}Tb_{0.25}Ba_2Cu_3O_7$ , the pre-onset temperatures are about 128 K and 123 K respectively. Figure 6A suggests that this temperature (for  $Tb_1Ba_2Cu_3O_7$ ) should be 136 K. The data from Ref. 12 on  $Y_{1-x}Ce_xBa_2Cu_3O_7$  indicate a pre-onset temperature for  $x=0.2$  a value of about 90 K where Figure 6A suggests for  $x=1.0$  a value of about 96 K. These results thus correlate very well with our study.

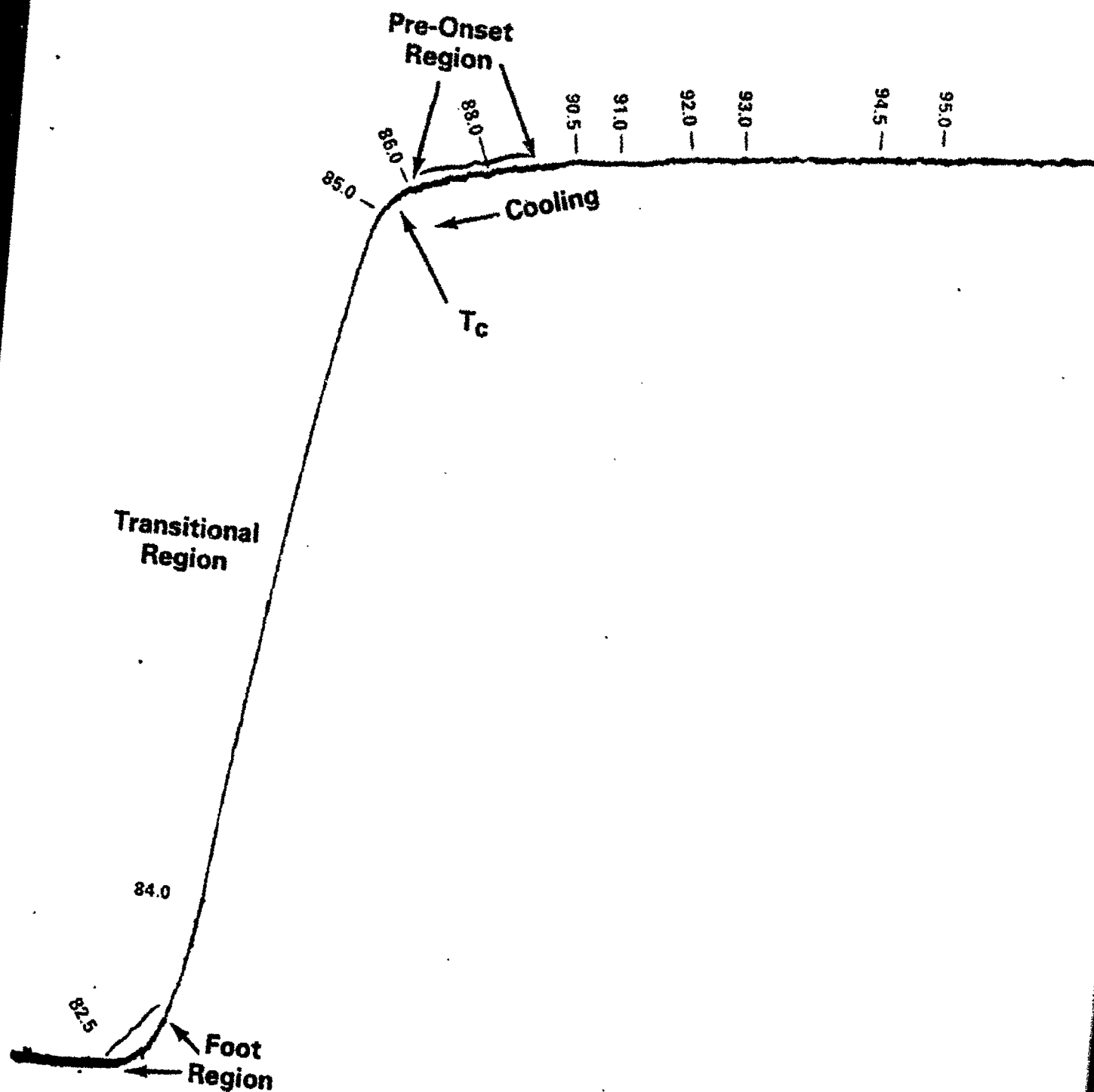


Figure 1A. The R versus T curve at  $B = 0$  for  $Y_{0.5}Gd_{0.5}Ba_2Cu_3O_{7-d}$  showing the pre-onset, transitional, and foot regions.

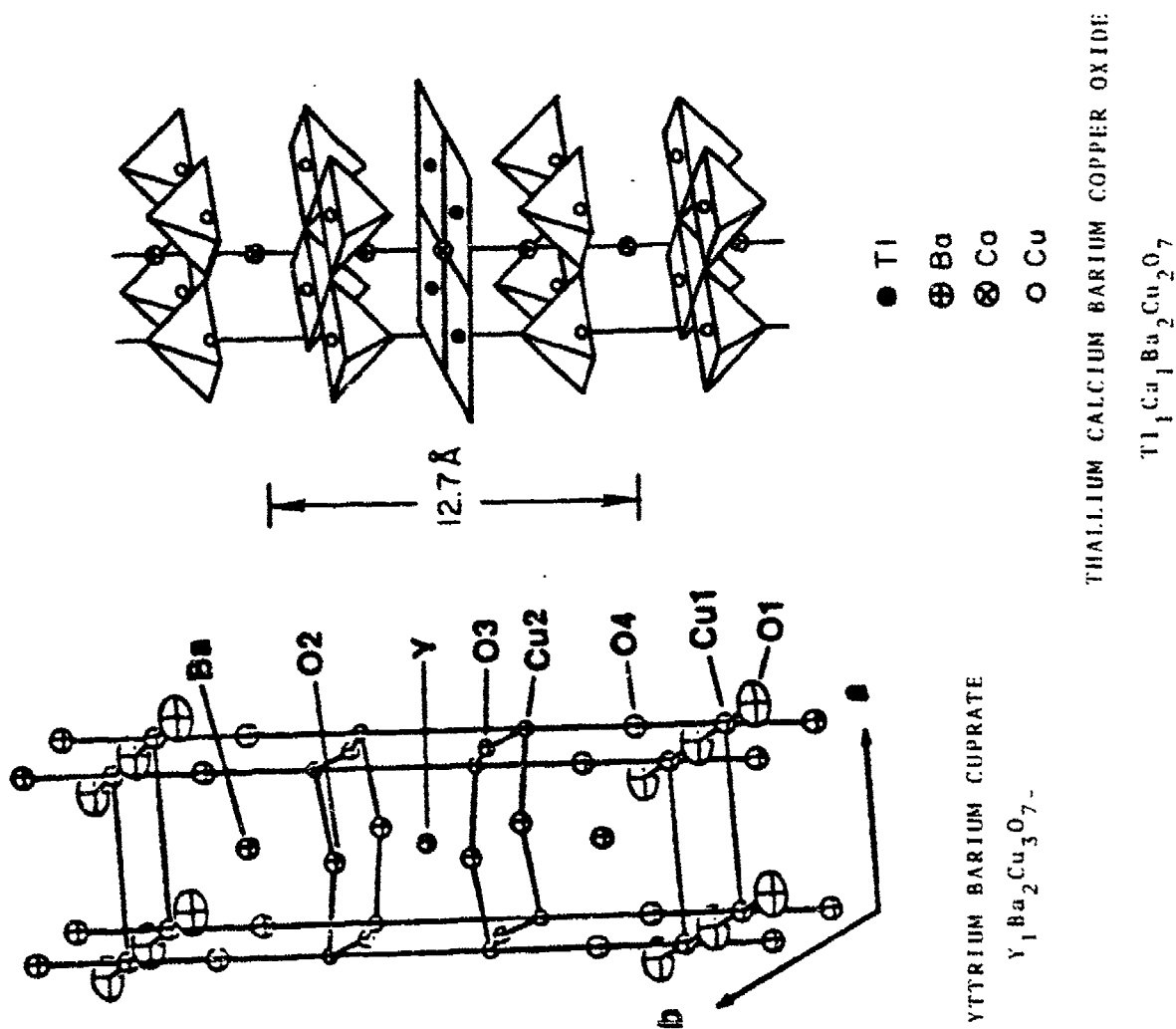
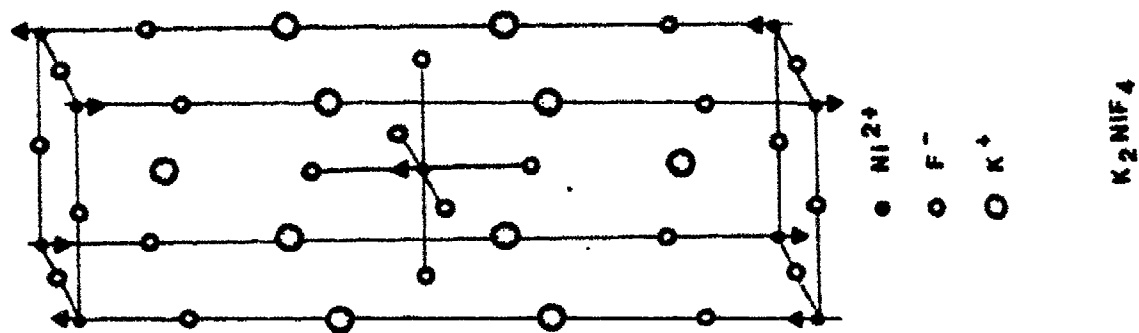


Figure 1B. The crystal structure of  $\text{Y}_1\text{Ba}_2\text{Cu}_3\text{O}_{7-x}$ , and related structures showing similarity of building blocks.

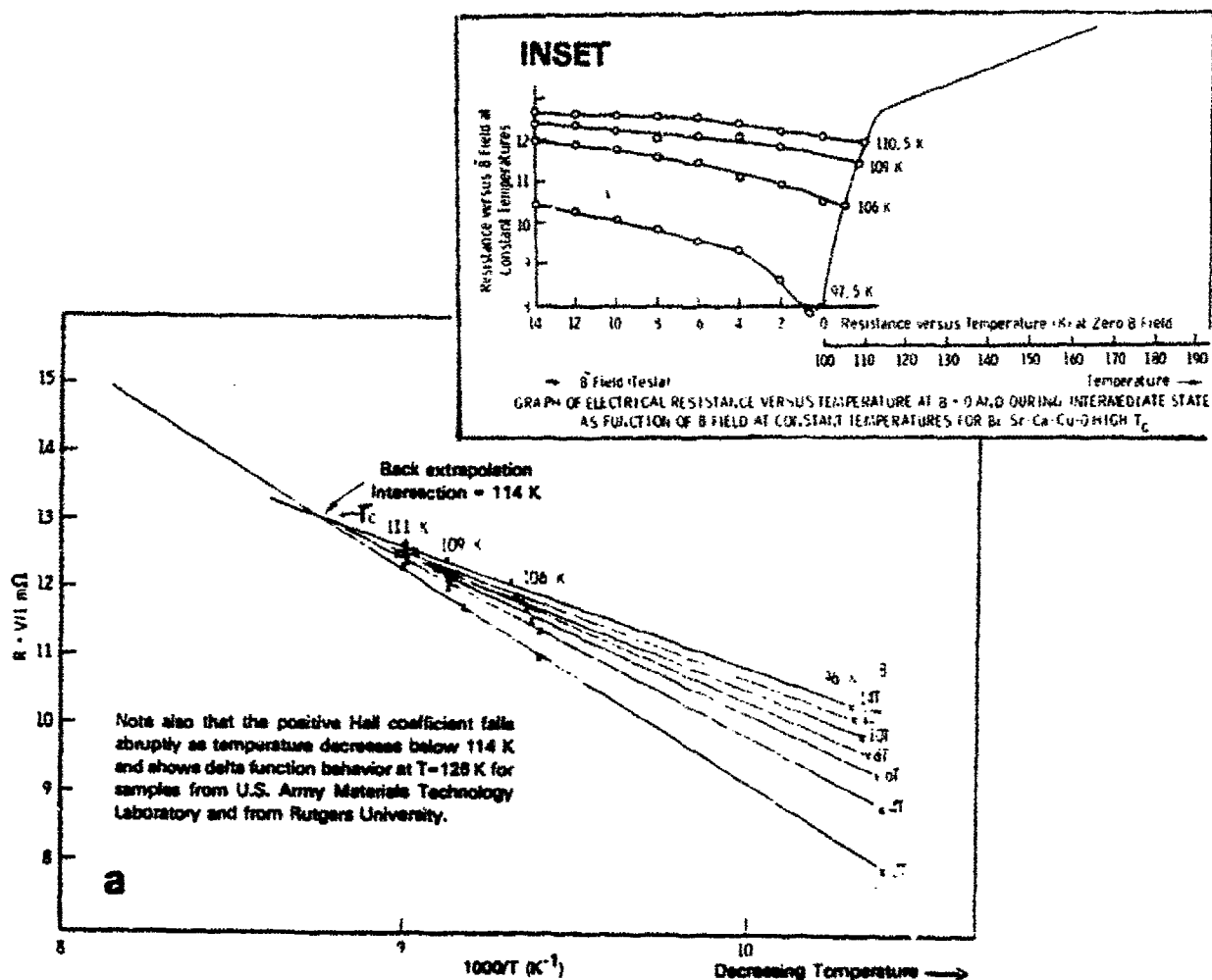


Figure 2A. Electrical resistance in milliohms versus inverse absolute temperature as affected by applied magnetic field. Data taken from transitional region shown in the inset. Note extrapolation intersection at 114 K.

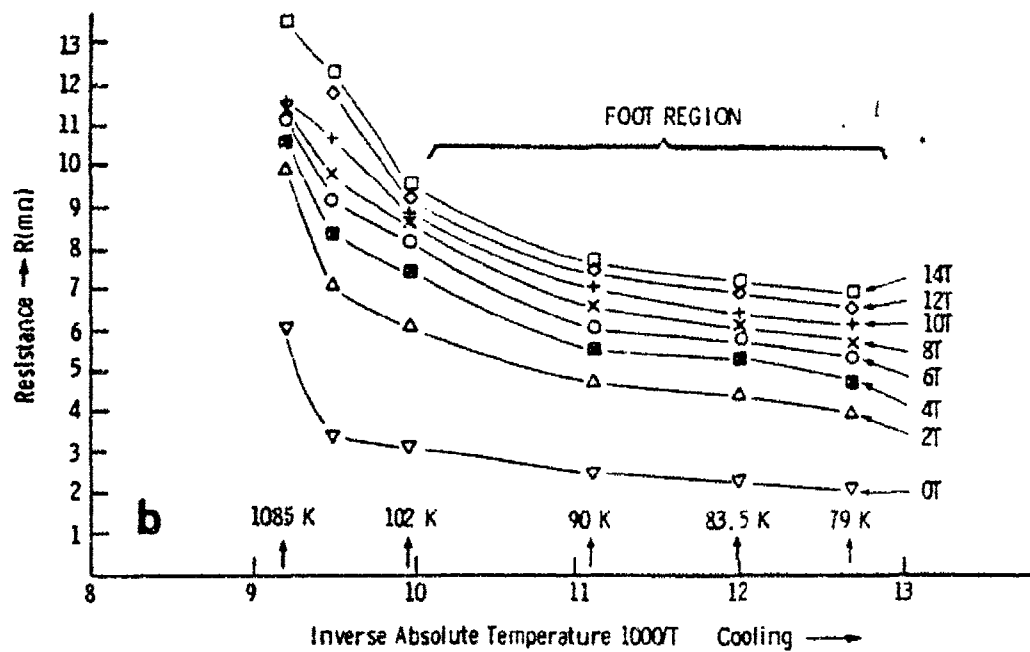


Figure 2B. Electrical resistance in milliohms versus inverse absolute temperature as affected by applied magnetic field in foot region.

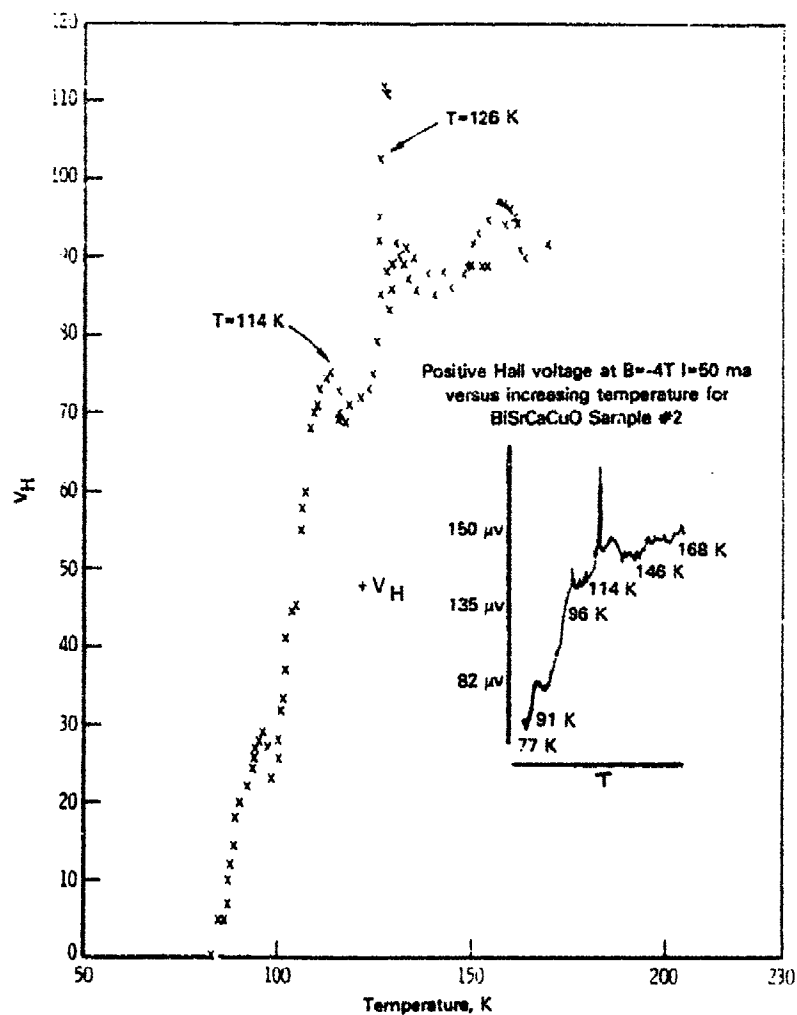
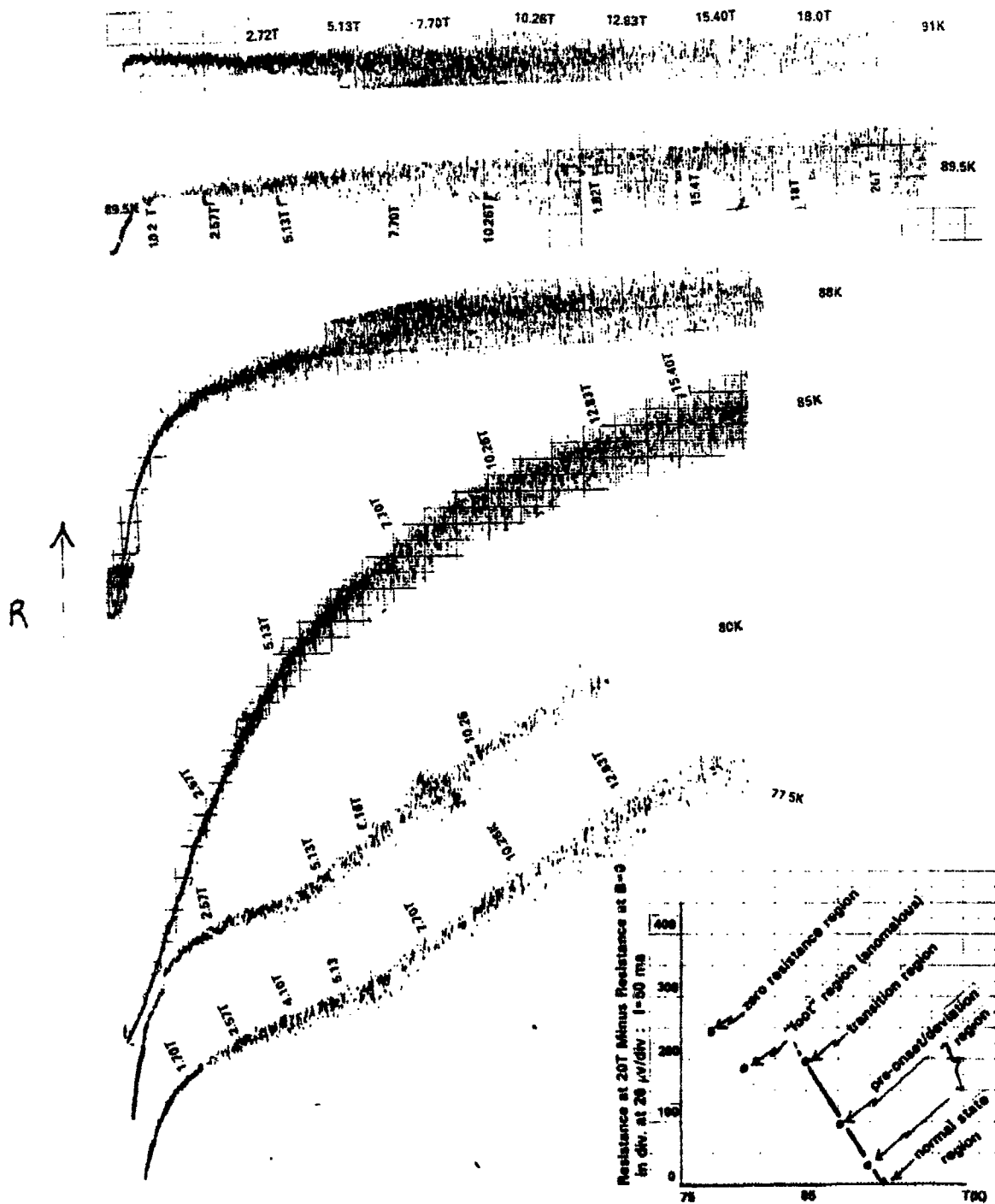


Figure 3. Hall voltage versus temperature for  $\text{Bi}_2\text{Sr}_2\text{Ca}_2\text{Cu}_3\text{O}_{10}$ . (Inset shows continuous measurements). Note sharp drop-off of positive Hall voltage at 114 K. (The delta function peaked behavior is discussed elsewhere, Ref. 4 and 5).



Change in Resistance vs B - Field at Temperatures from Normal State to Zero Resistance State: Up - Field, Sweep 20T in 60 sec;  $\Delta R$  in div at 20  $\mu\text{V/div}$  using 50 ma.

Figure 4. Graph of electrical resistance versus magnetic field sweep for various constant temperatures, showing that at  $T > T_0$  there is virtually zero response of the resistance to the electric field. The inset shows the change in resistance between  $B_{\text{max}}$  and  $B=20\text{T}$  as a function of temperature for 60 sec full field sweeps.

Potential (Microvolts/50ma) vs. 1000/T in Inverse Degrees K

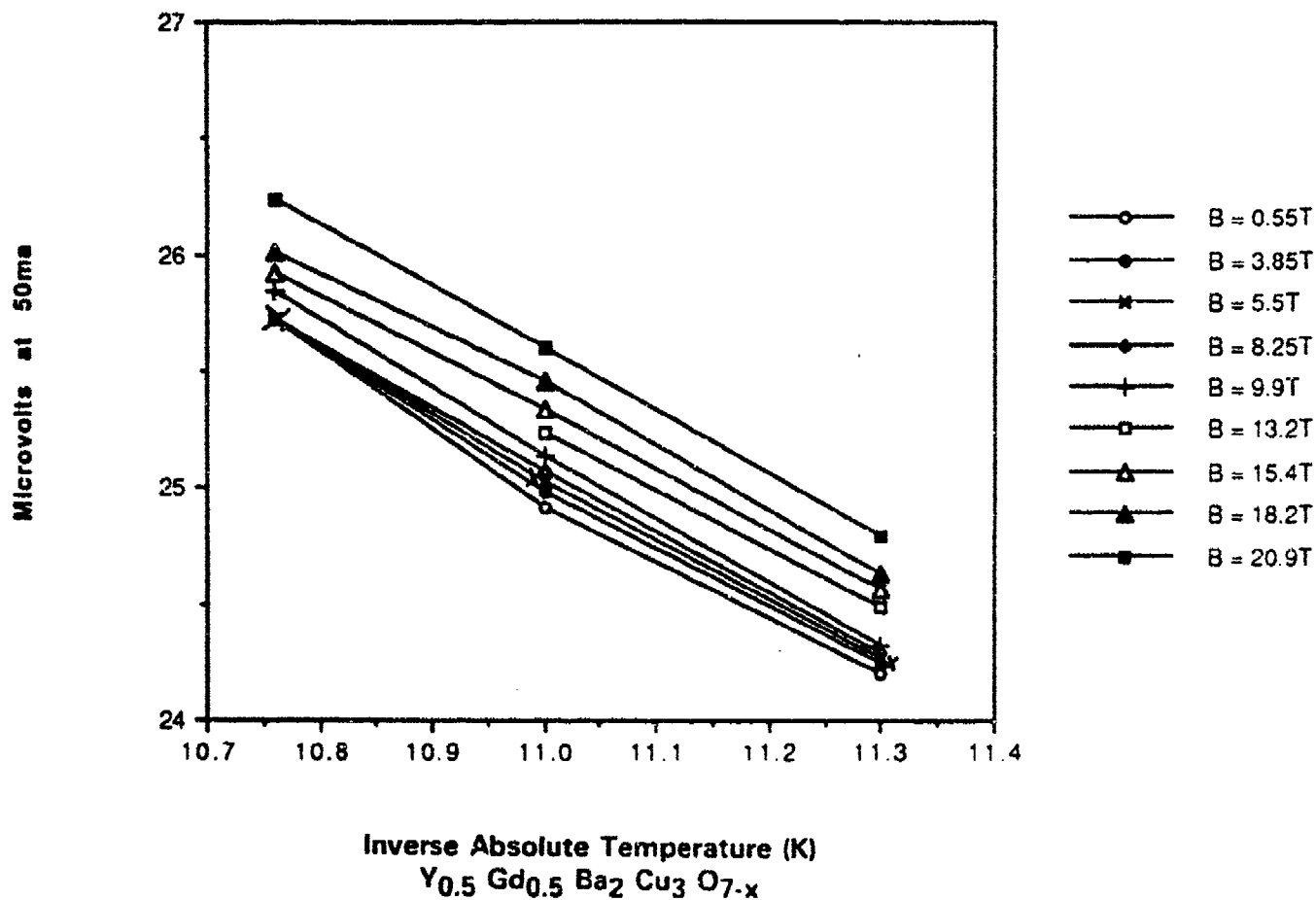


Figure 5. Graph of electrical resistance versus 1000/T data for the pre-onset region as affected by the applied magnetic field. Note the parallel character as contrasted to the converging character at  $T_c$  of Figures 2A and 2B.



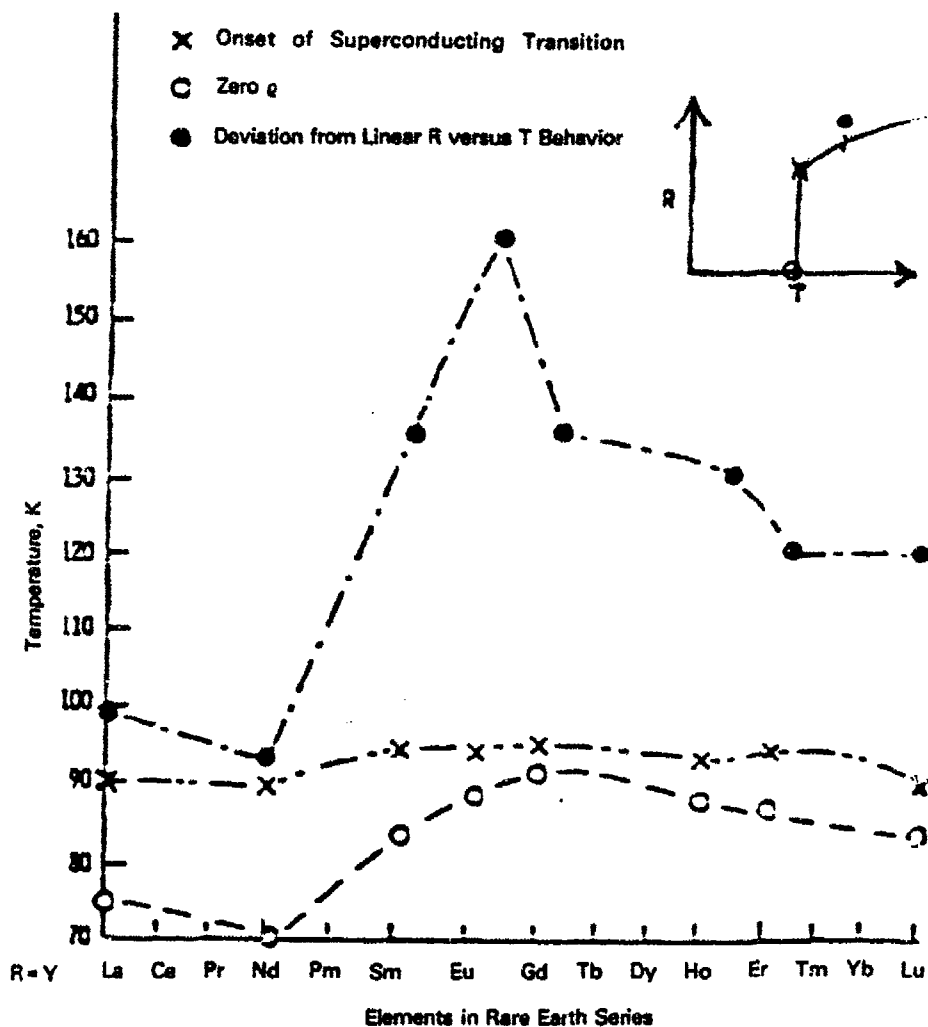


Figure 6A. The elevation of the pre-onset temperature and the zero resistance temperature as a function of the rare earth substituted for Y in  $Y_1Ba_2Cu_3O_{7-\delta}$ . Peak near Eu and Gd corresponds to peak in spin. Anomaly near Dy and Ho corresponds to peak in effective magnetic moment, data are from Ref. 2.

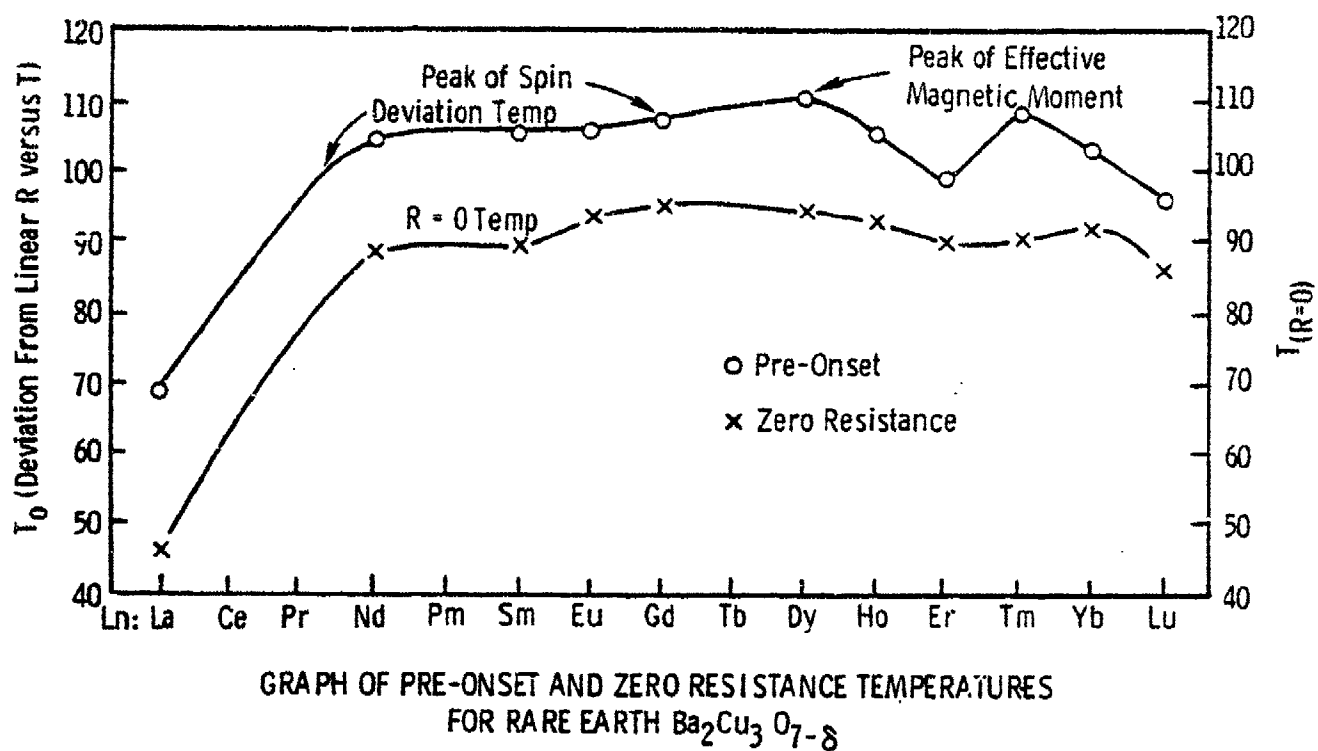


Figure 6B. Similar form of results as in Figure 6A but employing that data of Ref. 7.

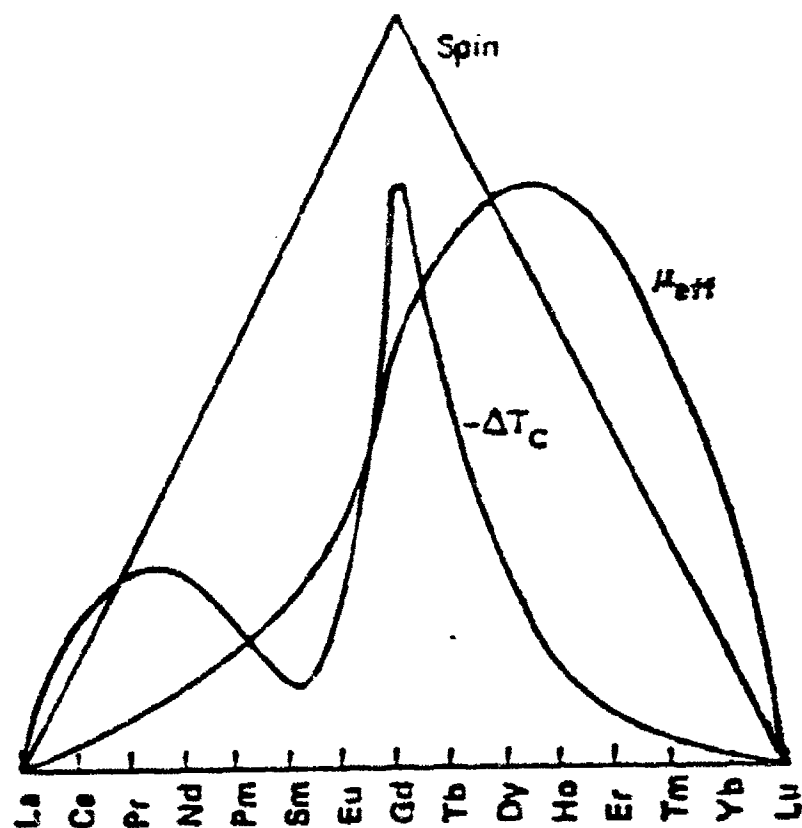


Figure 6C. The depression of  $T_c$  corresponding to different rare earths added (as dopant) to lanthanum. Effect is due to the influence of the paramagnetic moment of rare earths which causes scission of Cooper pairs, Ref. 8.

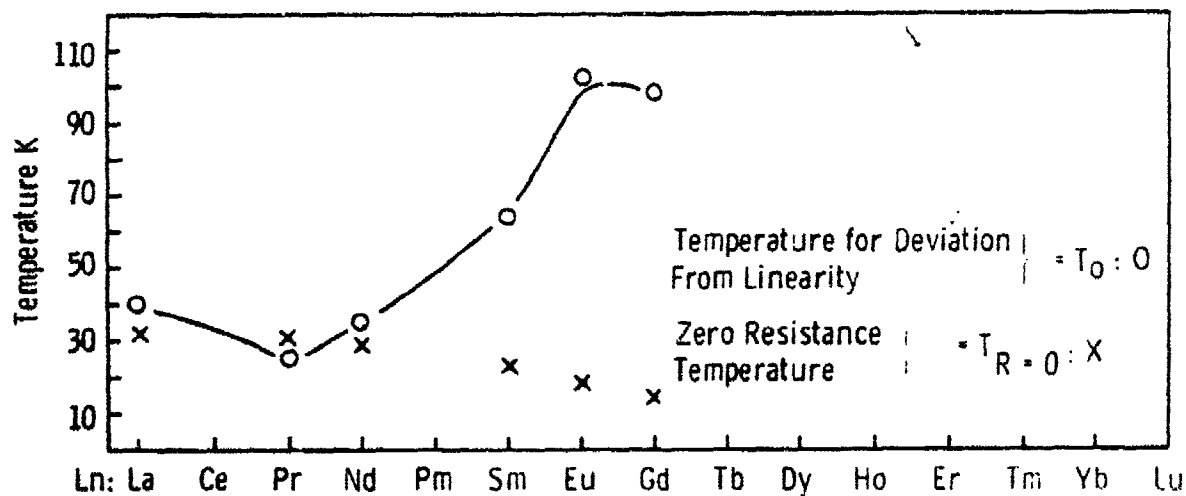


Figure 6D. Elevation of  $T_0$  but depression of  $T_{R=0}$  caused by addition or substitution of rare earth (lanthanide) in  $\text{La}_{1.6}\text{Sr}_{0.2}(\text{R.E. or Ln})_{0.2}\text{CuO}_4$ , Ref. 9.

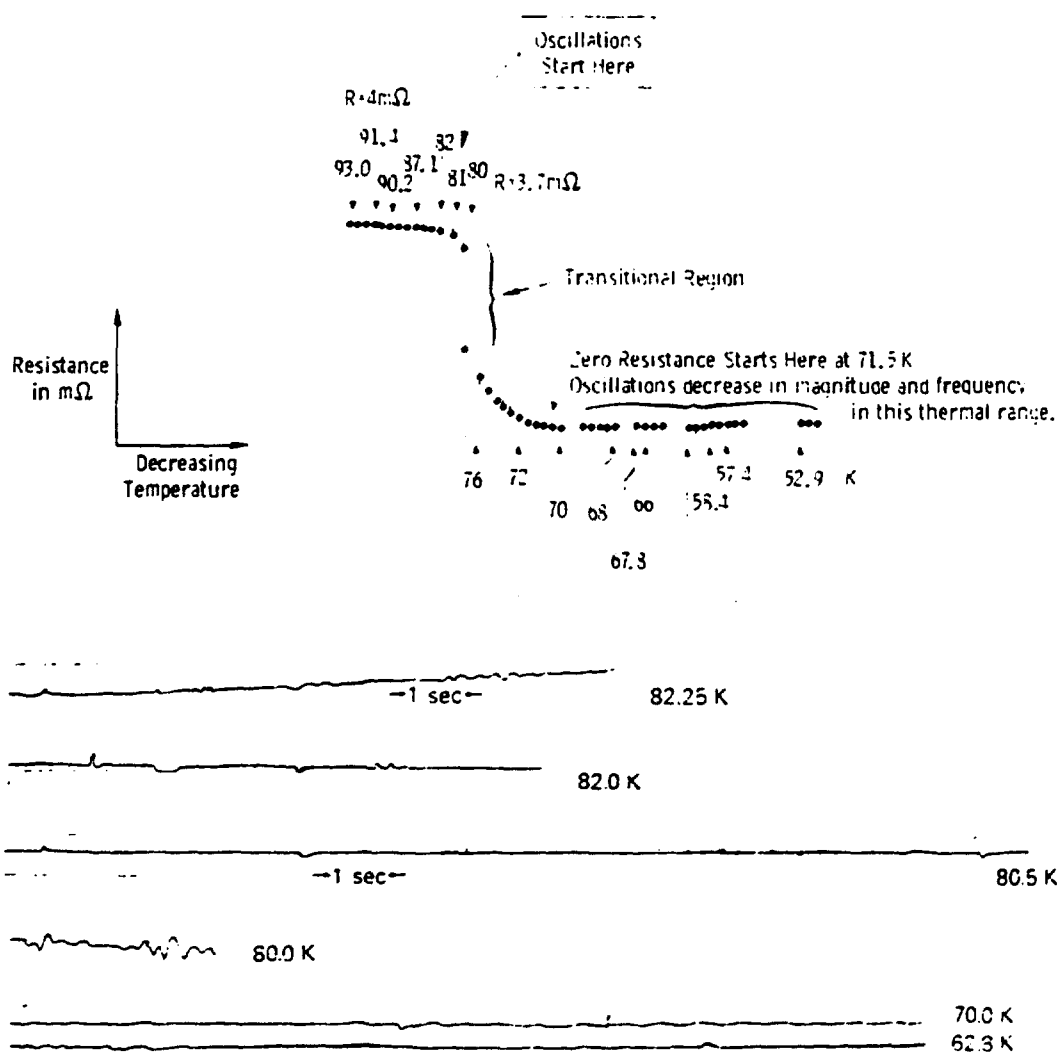


Figure 7. Upper: The  $R$  versus  $T$  curve of  $Y_1Ba_2Cu_3O_{7-\delta}$  showing small oscillations (in resistance versus time at constant temperature; vertical bars) commencing at the temperature at which deviation from linearity begins. Lower: Typical traces of small oscillation clusters at various temperatures in  $Y_1Ba_2Cu_3O_{7-\delta}$  (frequency  $\approx 0.1-10\text{Hz}$ ).

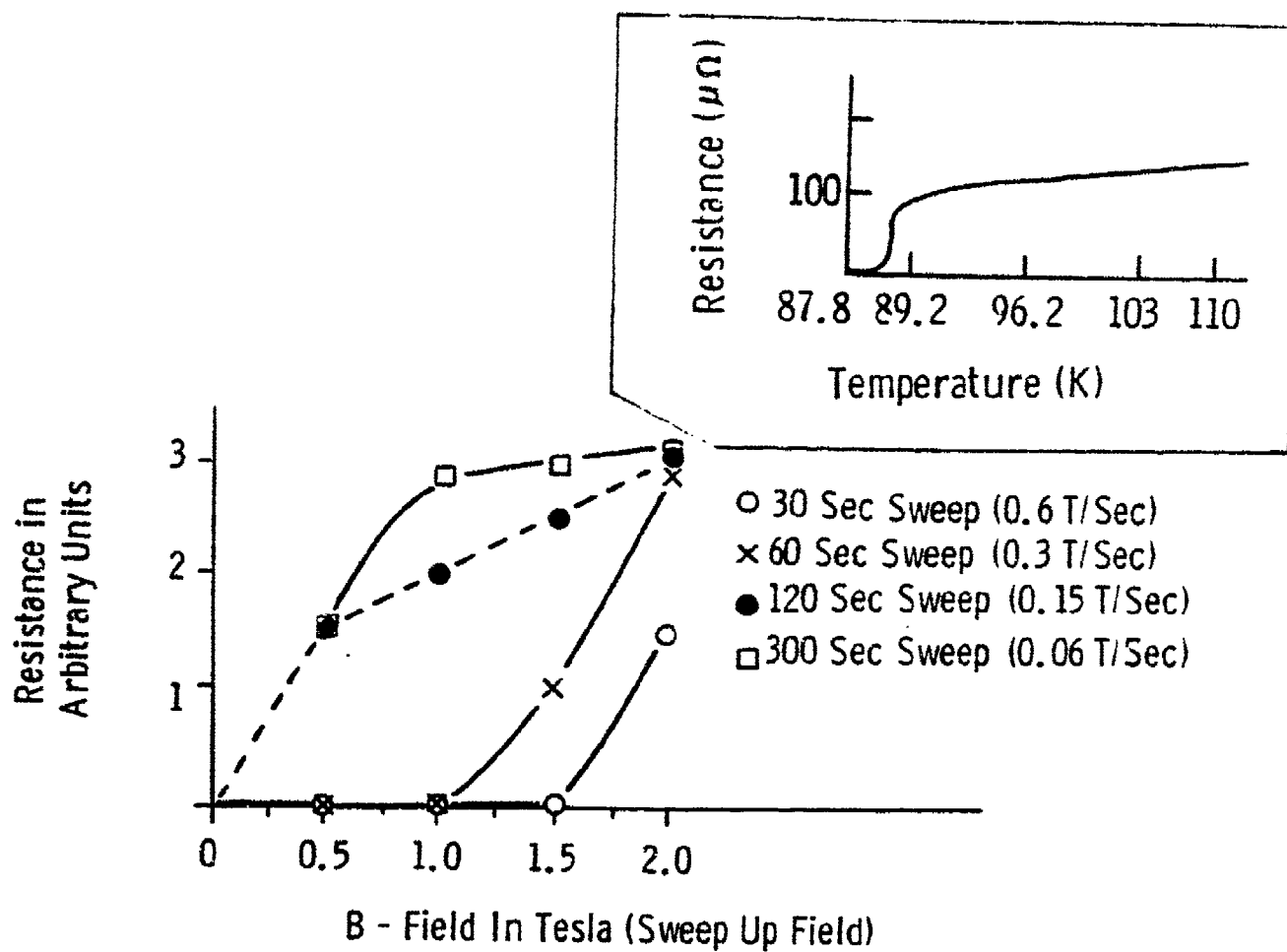


Figure 8. Time-dependence of recovering resistance of superconducting  $\text{Y}_1\text{Ba}_2\text{Cu}_{3-x}\text{Ga}_x\text{O}_{7-\delta}$  as a function of magnetic field sweep rate.

## REFERENCES

1. BEDNORZ, J.G., and MUELLER, R.A., Z. Phys. B64, 1986, p. 189.
2. CHU, C.W., HOR, R.H., MENG, R.L., GAO, L., HUANG, E.J., and WANG, Y.Q., Phys. Rev. Lett 58, 1987, p. 405; CHU, C.W., Phys. Rev. Lett 58, 1987, p. 1891.
3. a. JONES, T.E. et al., ACS Symposium Series 377, 1988, p. 155-167.  
 b. BRANDT, B., private communication; SAMPLE, H., BRANDT, B., and RUBIN, L., Rev. Sci. Instrum, v. 53, no. 8, 1982, p. 1129; BRANDT, B., RUBIN, L., and SAMPLE, H., Rev. Sci. Instrum, v. 59, no. 4, 1988, p. 642.  
 c. GOLDFARB, L., and CHEN, D.K., J. Appl. Phys., v. 63, 1988, p. 400; EKIN, J., LARSON, T.M., BERGEN, N.F., NELSON, A.J., SWARTZLANDER, A.B., KAZMERSKI, L.L., PANSON, A.J., and BLANKENSHIP, B.A. Appl. Phys. Lett 52, no. 21, 1988, p. 1819; EKIN, J., PANSON, A.J., and BLANKENSHIP, B.A., Appl. Phys. Lett 52, no. 4, 1988, p. 331.  
 d. MOON, B.M., J. Appl. Phys. (in press).
4. VEZZOLI, G.C., CHEN, M.F., CRAVER, F., SAFARI, A., MOON, B.M., LALEVIC, B., BURKE, T., and SHOGA, M., J. Magn. and Magn. Mat., v. 88, 1990, p. 351.
5. HUNDLEY, M.F., ZETTL, A., STACEY, A., and COHEN, M.L., Phys. Rev. B, v. 35, 1987, p. 8800; VEZZOLI, G.C., BURKE, T., MOON, B.M., LALEVIC, B., SAFARI, A., SUNDAR, H.G.K., BONOMETTI, R., ALEXANDER, C., RAU, C., and WATERS, K., J. Magn. and Magn. Mat. v. 79, 1989, p. 146; ZHAO, Y., XIA, J., HE, Z., SUN, S., ZHANG, Q., QIAN, Y., CHEN, Z., and PAN, G., Chin. Phys. Lett 5, 1988, p. 221; VEZZOLI, G.C., CHEN, M.F., CRAVER, F., and BURKE, T., Proc. New York Acad. Sci., "Frontiers in Physics;" SESHADRI, A., Univ. Miami Conf. on High-T<sub>c</sub> Mechanism, Plenum Press, N.Y. (in press).
6. VEZZOLI, G.C., J. Magn. and Magn. Mat., v. 82, 1989, p. 335.
7. MAPLE, M.B., DALICHAOUCH, Y., FERREIRA, J.M., KAKE, R.R., LEE, B.W., NEUMEIER, J.J., TORIKACHOILI, M.S., and KURVZ, K.N., Physica. B, v. 148, 1987, p. 155.
8. MATTHIES, B., SUHL, H., and CORENZWIT, E., J. Phys. and Chem. Solids, v. 13, no. 156, 1959, and Phys. Rev. Lett 1, 1958, p. 92.
9. TARASON, J.M., GREENE, L.H., MCKINNON, W.R., and HULL, G.W., Solid State Commun., v. 63, 1987, p. 499; MAPLE, M.B., DALICHAOUSCH, Y., FERREIRA, J.M., HAKE, R.R., LEW, B.W., NEUMEIER, J.J., TORIKACHOILI, M.S., YANG, K.N., ZHOU, H., GUERTIN, R.P., and KURIC, M.V., Physica B, v. 148, 1987, p. 155.
10. LALEVIC, B., J. Appl. Phys, v. 31, 1960, p. 234, and Phys. Rev., v. 128, 1964, p. 1070; WEBER, R., Phys. Rev., v. 72, 1947, p. 1241; KAPLAN, B., and DAUNT, J.G., Phys. Rev., v. 89, 1953, p. 907; BAIRD, D., Can. J. Phys., v. 37, 1959, p. 120; ANDREWS, D.H., MITTON, R.M., and DESORBO, W., J. Opt. Soc. Am, v. 36, 1946, p. 520, and Proc. Roy. Soc. (London) A-82, v. 194, 1948.
11. MOON, B.M. The Univ. of Illinois, private communications.
12. FINDER, C., and BLANCHET, G.B., Phys. Rev. Lett 67, no. 20, 1991, p. 2902.

# DISTRIBUTION LIST

No. of Copies	To
1	Office of the Under Secretary of Defense for Research and Engineering, The Pentagon, Washington, DC 20301
	Commander, U.S. Army Laboratory Command, 2800 Powder Mill Road, Adelphi, MD 20783-1145
1	ATTN: AMSLC-IM-TL
1	AMSLC-CT
	Commander, Defense Technical Information Center, Cameron Station, Building 5, 5010 Duke Street, Alexandria, VA 22304-6145
2	ATTN: DTIC-FDAC
1	MIA/CINDAS, Purdue University, 2595 Yeager Road, West Lafayette, IN 47905
	Commander, Army Research Office, P.O. Box 12211, Research Triangle Park, NC 27709-2211
1	ATTN: Information Processing Office
	Commander, U.S. Army Materiel Command, 5001 Eisenhower Avenue, Alexandria, VA 22333
1	ATTN: AMCSCI
	Commander, U.S. Army Materiel Systems Analysis Activity, Aberdeen Proving Ground, MD 21005
1	ATTN: AMXSY-MP, H. Cohen
	Commander, U.S. Army Missile Command, Redstone Scientific Information Center, Redstone Arsenal, AL 35898-5241
1	ATTN: AMSMI-RD-CS-R/Doc
1	AMSMI-RLM
	Commander, U.S. Army Armament, Munitions and Chemical Command, Dover, NJ 07801
2	ATTN: Technical Library
	Commander, U.S. Army Natick Research, Development and Engineering Center, Natick, MA 01760-5010
1	ATTN: Technical Library
	Commander, U.S. Army Satellite Communications Agency, Fort Monmouth, NJ 07703
1	ATTN: Technical Document Center
	Commander, U.S. Army Tank-Automotive Command, Warren, MI 48397-5000
1	ATTN: AMSTA-ZSK
1	AMSTA-TSL, Technical Library
	Commander, White Sands Missile Range, NM 88002
1	ATTN: STEWS-WS-VT
	President, Airborne, Electronics and Special Warfare Board, Fort Bragg, NC 28307
1	ATTN: Library
	Director, U.S. Army Ballistic Research Laboratory, Aberdeen Proving Ground, MD 21005
1	ATTN: SLCBR-TSB-S (STINFO)
	Commander, Dugway Proving Ground, UT 84022
1	ATTN: Technical Library, Technical Information Division
	Commander, Harry Diamond Laboratories, 2800 Powder Mill Road, Adelphi, MD 20783
1	ATTN: Technical Information Office
	Director, Benet Weapons Laboratory, LCWSL, USA AMCCOM, Watervliet, NY 12189
1	ATTN: AMSMC-LCB-TL
1	AMSMC-LCB-R
1	AMSMC-LCB-RM
1	AMSMC-LCB-RP
	Commander, U.S. Army Foreign Science and Technology Center, 220 7th Street, N.E., Charlottesville, VA 22901-5396
3	ATTN: AIFRTC, Applied Technologies Branch, Gerald Schlesinger
	Commander, U.S. Army Aeromedical Research Unit, P.O. Box 577, Fort Rucker, AL 36360
1	ATTN: Technical Library

No. of Copies	To
1	Commander, U.S. Army Aviation Systems Command, Aviation Research and Technology Activity, Aviation Applied Technology Directorate, Fort Eustis, VA 23604-5577 ATTN: SAVDL-E-MOS
1	U.S. Army Aviation Training Library, Fort Rucker, AL 36360 ATTN: Building 5906-5907
1	Commander, U.S. Army Agency for Aviation Safety, Fort Rucker, AL 36362 ATTN: Technical Library
1	Commander, USACDC Air Defense Agency, Fort Bliss, TX 79916 ATTN: Technical Library
1	Commander, Clarke Engineer School Library, 3202 Nebraska Ave., N. Ft. Leonard Wood, MO 65473-5000 ATTN: Library
1	Commander, U.S. Army Engineer Waterways Experiment Station, P.O. Box 631, Vicksburg, MS 39180 ATTN: Research Center Library
1	Commandant, U.S. Army Quartermaster School, Fort Lee, VA 23801 ATTN: Quartermaster School Library
1	Naval Research Laboratory, Washington, DC 20375 ATTN: Code 5830
2	Dr. G. R. Yoder - Code 6384
1	Chief of Naval Research, Arlington, VA 22217 ATTN: Code 471
1	Edward J. Morrissey, WRDC/MLTE, Wright-Patterson Air Force Base, OH 45433-6523
1	Commander, U.S. Air Force Wright Research & Development Center, Wright-Patterson Air Force Base, OH 45433-6523 ATTN: WRDC/MLLP, M. Forney, Jr.
1	WRDC/MLBC, Mr. Stanley Schulman
1	NASA - Marshall Space Flight Center, MSFC, AL 35812 ATTN: Mr. Paul Schuerer/EH01
1	U.S. Department of Commerce, National Institute of Standards and Technology, Gaithersburg, MD 20899 ATTN: Stephen M. Hsu, Chief, Ceramics Division, Institute for Materials Science and Engineering
1	Committee on Marine Structures, Marine Board, National Research Council, 2101 Constitution Avenue, N.W., Washington, DC 20418
1	Materials Sciences Corporation, Suite 250, 500 Office Center Drive, Fort Washington, PA 19034-3213
1	Charles Stark Draper Laboratory, 68 Albany Street, Cambridge, MA 02139
1	Wyman-Gordon Company, Worcester, MA 01601 ATTN: Technical Library
1	General Dynamics, Convair Aerospace Division P.O. Box 748, Fort Worth, TX 76101 ATTN: Mfg. Engineering Technical Library
1	Plastics Technical Evaluation Center, PLASTEC, ARDEC Bldg. 355N, Picatinny Arsenal, NJ 07806-5000 ATTN: Harry Peibly
1	Department of the Army, Aerostructures Directorate, MS-266, U.S. Army Aviation R&T Activity - AVSCOM, Langley Research Center, Hampton, VA 23665-5225
1	NASA - Langley Research Center, Hampton, VA 23665-5225
1	U.S. Army Propulsion Directorate, NASA Lewis Research Center, 2100 Brookpark Road, Cleveland, OH 44135-3191
1	NASA - Lewis Research Center, 2100 Brookpark Road, Cleveland, OH 44135-3191
2	Director, U.S. Army Materials Technology Laboratory, Watertown, MA 02172-0001 ATTN: SLCMT-TML
5	Authors



U.S. Army Materials Technology Laboratory  
Watertown, Massachusetts 02172-0001

THE PRE-ONSET, TRANSITIONAL, AND FOOT REGIONS  
IN RESISTANCE VERSUS TEMPERATURE BEHAVIOR IN  
HIGH- $T_c$  CUPRATES: INFERENCES REGARDING  
MAXIMUM  $T_c$  - G. C. Vezzoli, T. Burke, M. F. Chen  
F. Craver, and W. Stanley

Technical Report MTL TR 92-67, September 1992,  
20 pp - illustrations

AD

UNCLASSIFIED  
UNLIMITED DISTRIBUTION

Key Words  
Superconductivity  
Supercurrent  
Cooper pairs

We have studied the pre-onset deviation-from-linearity region, the transitional regime, and the foot region in the resistance versus temperature behavior of high- $T_c$  oxide superconductors, employing time varying magnetic fields and carefully controlled precise temperatures. We have shown that the best value of  $T_c$  can be extrapolated from the magnetic field induced divergence of the resistance versus inverse absolute temperature data as derived from the transitional and/or foot regions. These data are in accord with results from previous Hall effect studies. The pre-onset region however, shows a differing behavior (in R versus 1000/T as a function of B) which we believe links it to an incipient Cooper pairing that suffers a kinetic barrier opposing formation of a full supercurrent. This kinetic dependence is believed to be associated with the lifetime of the mediator particle. This particle is interpreted to be the virtual exciton formed from internal-field induced charge-transfer excitations which transiently neutralize the multivalence cations and establish bound holes on the oxygens.

U.S. Army Materials Technology Laboratory  
Watertown, Massachusetts 02172-0001

THE PRE-ONSET, TRANSITIONAL, AND FOOT REGIONS  
IN RESISTANCE VERSUS TEMPERATURE BEHAVIOR IN  
HIGH- $T_c$  CUPRATES: INFERENCES REGARDING  
MAXIMUM  $T_c$  - G. C. Vezzoli, T. Burke, M. F. Chen  
F. Craver, and W. Stanley

Technical Report MTL TR 92-67, September 1992,  
20 pp - illustrations

AD

UNCLASSIFIED  
UNLIMITED DISTRIBUTION

Key Words  
Superconductivity  
Supercurrent  
Cooper pairs

We have studied the pre-onset deviation-from-linearity region, the transitional regime, and the foot region in the resistance versus temperature behavior of high- $T_c$  oxide superconductors, employing time varying magnetic fields and carefully controlled precise temperatures. We have shown that the best value of  $T_c$  can be extrapolated from the magnetic field induced divergence of the resistance versus inverse absolute temperature data as derived from the transitional and/or foot regions. These data are in accord with results from previous Hall effect studies. The pre-onset region however, shows a differing behavior (in R versus 1000/T as a function of B) which we believe links it to an incipient Cooper pairing that suffers a kinetic barrier opposing formation of a full supercurrent. This kinetic dependence is believed to be associated with the lifetime of the mediator particle. This particle is interpreted to be the virtual exciton formed from internal-field induced charge-transfer excitations which transiently neutralize the multivalence cations and establish bound holes on the oxygens.

U.S. Army Materials Technology Laboratory  
Watertown, Massachusetts 02172-0001

THE PRE-ONSET, TRANSITIONAL, AND FOOT REGIONS  
IN RESISTANCE VERSUS TEMPERATURE BEHAVIOR IN  
HIGH- $T_c$  CUPRATES: INFERENCES REGARDING  
MAXIMUM  $T_c$  - G. C. Vezzoli, T. Burke, M. F. Chen  
F. Craver, and W. Stanley

Technical Report MTL TR 92-67, September 1992,  
20 pp - illustrations

AD

UNCLASSIFIED  
UNLIMITED DISTRIBUTION

Key Words  
Superconductivity  
Supercurrent  
Cooper pairs

We have studied the pre-onset deviation-from-linearity region, the transitional regime, and the foot region in the resistance versus temperature behavior of high- $T_c$  oxide superconductors, employing time varying magnetic fields and carefully controlled precise temperatures. We have shown that the best value of  $T_c$  can be extrapolated from the magnetic field induced divergence of the resistance versus inverse absolute temperature data as derived from the transitional and/or foot regions. These data are in accord with results from previous Hall effect studies. The pre-onset region however, shows a differing behavior (in R versus 1000/T as a function of B) which we believe links it to an incipient Cooper pairing that suffers a kinetic barrier opposing formation of a full supercurrent. This kinetic dependence is believed to be associated with the lifetime of the mediator particle. This particle is interpreted to be the virtual exciton formed from internal-field induced charge-transfer excitations which transiently neutralize the multivalence cations and establish bound holes on the oxygens.

U.S. Army Materials Technology Laboratory  
Watertown, Massachusetts 02172-0001

THE PRE-ONSET, TRANSITIONAL, AND FOOT REGIONS  
IN RESISTANCE VERSUS TEMPERATURE BEHAVIOR IN  
HIGH- $T_c$  CUPRATES: INFERENCES REGARDING  
MAXIMUM  $T_c$  - G. C. Vezzoli, T. Burke, M. F. Chen  
F. Craver, and W. Stanley

Technical Report MTL TR 92-67, September 1992,  
20 pp - illustrations

AD

UNCLASSIFIED  
UNLIMITED DISTRIBUTION

Key Words  
Superconductivity  
Supercurrent  
Cooper pairs

We have studied the pre-onset deviation-from-linearity region, the transitional regime, and the foot region in the resistance versus temperature behavior of high- $T_c$  oxide superconductors, employing time varying magnetic fields and carefully controlled precise temperatures. We have shown that the best value of  $T_c$  can be extrapolated from the magnetic field induced divergence of the resistance versus inverse absolute temperature data as derived from the transitional and/or foot regions. These data are in accord with results from previous Hall effect studies. The pre-onset region however, shows a differing behavior (in R versus 1000/T as a function of B) which we believe links it to an incipient Cooper pairing that suffers a kinetic barrier opposing formation of a full supercurrent. This kinetic dependence is believed to be associated with the lifetime of the mediator particle. This particle is interpreted to be the virtual exciton formed from internal-field induced charge-transfer excitations which transiently neutralize the multivalence cations and establish bound holes on the oxygens.